Available online at www.sciencedirect.com
SCIENCE DIRECT
Quaternary International 150 (2006) 95–102

Simulation of the Holocene climate evolution in Northern Africa: The termination of the African Humid Period

H. Renssen[a,*], V. Brovkin[b], T. Fichefet[c], H. Goosse[c]

[a]Faculty of Earth and Life Sciences, Vrije Universiteit Amsterdam, De Boelelaan 1085, NL-1081HV Amsterdam, The Netherlands
[b]Postdam Institut für Klimafolgenforschung, Postfach 601203, D-14412 Potsdam, Germany
[c]Institut d'Astronomie et de Géophysique Georges Lemaître, Université catholique de Louvain, Chemin du Cyclotron 2, B-1348 Louvain-la-Neuve, Belgium

Available online 13 March 2006

Abstract

The Holocene climate evolution in Northern Africa is studied in a 9000-yr-long transient simulation with a coupled atmosphere–ocean–vegetation model forced by changes in insolation and atmospheric greenhouse gas concentrations. The model simulates in the monsoonal domains a significant decrease in precipitation under influence of the orbitally forced reduction in summer insolation. In the Western Sahara region, the simulated mid-Holocene transition from humid to arid conditions (the termination of the African Humid Period) is highly non-linear with the occurrence of centennial-scale climate fluctuations due to the biogeophysical feedback between precipitation and vegetation cover. This result is in agreement with proxy data from the Western Sahara region. The other monsoonal regions experience a more gradual climate evolution that linearly follows the insolation forcing, which appears in disagreement with available lake level records.

1. Introduction

It is well known that the climate in Northern Africa experienced pronounced changes during the course of the Holocene. Numerous paleoclimatic data show that the early-to-middle Holocene (~11.5–5.5 kyr cal BP, thousand calendar year before present) was a relatively humid period in Northern Africa. During this phase, often called the African Humid Period (AHP), grasslands covered the Sahara/Sahel region, and many lakes and wetlands existed here (Gasse, 2000; Prentice et al., 2000). The humid conditions at this time are associated with a relatively strong summer monsoon circulation, which in turn was due to an enhanced land–sea thermal contrast under influence of the relatively high summer insolation in the early Holocene (Kutzbach and Street-Perrott, 1985). Proxy evidence indicates that the AHP came to an abrupt end around 5.5 kyr cal BP (DeMenocal et al., 2000), despite the gradual nature of the insolation forcing.

The abruptness of the AHP termination is related to a non-linear, positive biogeophysical feedback between vegetation and precipitation in the Sahara region: when precipitation is reduced, the vegetation cover decreases, thereby increasing the surface albedo and radiative heat loss, which in turn leads to a decrease in precipitation (Charney, 1975; Charney et al., 1975). Previous climate model experiments have reproduced the abrupt termination of the AHP, thereby showing the effectiveness of this biogeophysical feedback (Claussen et al., 1999). The shift from a "green" Sahara state to a "desert" state around 5.5 kyr cal BP indicates that these two basic states can both be stable in the Sahara/Sahel region during the Holocene. This has been confirmed by model studies (Brovkin et al., 1998; Claussen, 1998). In addition, some proxy data give evidence of rapid centennial-scale fluctuations between these green and desert states during the termination phase of the AHP (Fabre and Petit-Maire, 1988; Lézine et al., 1990; Damnati, 2000), indicating that the dynamics of the coupled climate system are more complex than previously thought.

To study the climatic changes associated with the termination of the AHP in detail, we have conducted several numerical experiments with a coupled, three-dimensional climate model. In an earlier paper (Renssen

*Corresponding author. Tel.: +31 20 4447376; fax: +31 20 5989940.
E-mail address: hans.renssen@falw.geo.vu.nl (H. Renssen).

1040-6182/$ - see front matter © 2006 Elsevier Ltd and INQUA. All rights reserved.
doi:10.1016/j.quaint.2005.01.001

et al., 2003a), we discussed the simulated Holocene climatic evolution in the Western Sahara region, where the AHP termination is characterized by centennial-scale shifts between green and desert states under influence of Charney's (1975) biogeophysical feedback. Lake level data suggest that the mid-Holocene wet–dry transition was also abrupt in other regions within the monsoonal domain, such as Northeast Africa and West Asia (e.g., Gasse and Van Campo, 1994). In this paper, we therefore extend our previous study, particularly by considering the spatial characteristics of the simulated climatic changes. We address the following questions: What is the spatial extension of the unstable mid-Holocene phase in our simulation? How does the simulated AHP termination in the Western Sahara compare to the Holocene climatic evolution in other regions that are influenced by the summer monsoons?

2. Model and experimental design

We have performed the simulations of the AHP termination with version 2 of the ECBilt–CLIO coupled atmosphere–ocean model. The atmospheric component is ECBilt, an atmospheric model (T21 horizontal resolution, three layers) based on quasi-geostrophic equations (Opsteegh et al., 1998). As an extension to the quasi-geostrophic equations, an estimate of the neglected terms in the vorticity and thermodynamic equations is included as a temporally and spatially varying forcing. This forcing is calculated from the diagnostically derived vertical motion field and leads to a considerable improvement of the simulation of the Hadley Cell circulation, resulting in a better representation of the strength and position of the jet stream and transient eddy activity. ECBilt resolves synoptic variability associated with weather patterns. Weber (2001) and Weber et al. (2004) coupled this atmospheric component ECBilt to a flat-bottom ocean model to study the climate response to insolation forcing. We have applied a version in which ECBilt is coupled to CLIO, an oceanic general circulation model ($3^\circ \times 3^\circ$ latitude–longitude horizontal resolution, 19 layers in the vertical) coupled to a comprehensive dynamic–thermodynamic sea–ice model (Goosse and Fichefet, 1999). The ECBilt–CLIO model reproduces reasonably well the modern climate (Goosse et al., 2001; Renssen et al., 2002).

For the experiments on the AHP termination, we applied a version in which ECBilt–CLIO is coupled to VECODE, a model that describes the dynamics of grassland and forest, and desert as a third dummy type (Brovkin et al., 2002). In the version we applied, the coupling between VECODE and ECBilt is only through the surface albedo, thus neglecting the impact of vegetation on other aspects of climate (e.g., soil hydrology, carbon cycle). ECBilt–CLIO–VECODE was used earlier to investigate the impact of global deforestation on the long-term stability of the ocean thermohaline circulation (Renssen et al., 2003b). The Holocene climate evolution of the polar regions was recently investigated with a new version of the model (version 3, Renssen et al., 2005a, b). More information on the model and a complete list of references are available at http://www.knmi.nl/onderzk/CKO/ecbilt.html.

We studied the AHP termination in a 9000-yr-long experiment (Renssen et al., 2003a), forced with insolation (Berger, 1978) and atmospheric concentrations of CO_2 and CH_4 (Raynaud et al., 2000). The insolation changes represent the main forcing of the experiment, as the 9–0 kyr cal BP variations in atmospheric greenhouse gases are only responsible for a radiative forcing of about $\sim 0.5\,W/m^2$ (compared to $\sim 35\,W/m^2$ for June insolation in the Northern Hemisphere, Fig. 1a). All other boundary conditions (i.e., solar constant, other greenhouse gas

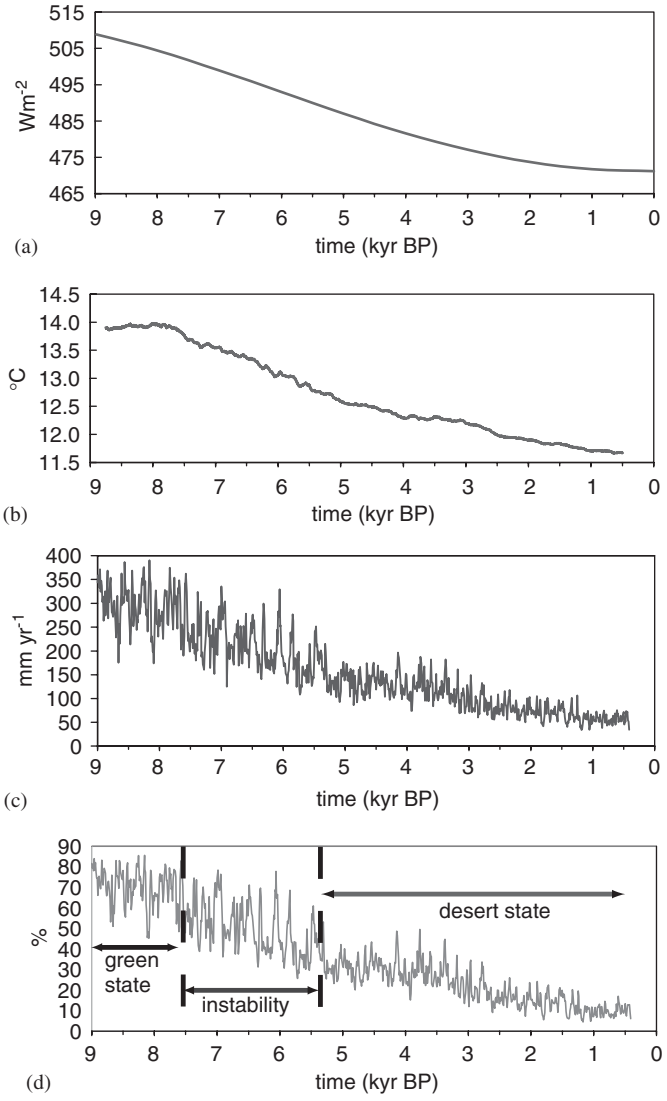

Fig. 1. Simulated climate evolution in Western Sahara region during the last 9000 yr: (a) June insolation in the Northern Hemisphere (W/m^2, main forcing), (b) land–sea thermal gradient (°C), shown here as the 500-yr running mean July surface temperature difference between two grid points (22°W, 3°N and 11°W, 19°N), (c) decadal mean precipitation (mm/yr) and (d) vegetation cover (%), both in the Western Sahara region (mean over 6 grid cells covering 14°W to 3°E, 17°N to 28°N).

concentrations, land–sea–ice distribution) were fixed at their 1750 AD values. The initial conditions were derived from an experiment in equilibrium with 9 kyr cal BP orbital forcing and greenhouse gas concentrations. In the latter experiment, grasslands covered most of the Sahara, in agreement with paleobotanical data.

3. Results and discussion

In the Western Sahara/Sahel region, the response of the model to the gradual decrease in summer insolation (Fig. 1a) can be separated in three distinct phases (Renssen et al., 2003a). During the first phase, lasting from 9 to 7.5 kyr cal BP, the climate in the Western Sahara/Sahel region is characterized by relatively high summer temperatures and enhanced precipitation (290 mm/yr, Fig. 1b and c), reflecting a relatively strong summer monsoon circulation. The vegetation cover has an average value of 70% (Fig. 1d), so that this phase can be typified as a "green state". This green state is associated with a relatively strong land–sea thermal gradient, leading to an increased transport of humid air towards the continent and enhanced convective precipitation over land. In the second phase (7.5–5.5 kyr cal BP), the annual mean precipitation and vegetation cover decrease to values of 210 mm/yr and 50%, respectively (Fig. 1). Furthermore, the variability in precipitation and vegetation cover increases significantly, with rapid fluctuations between 30% and 80% for the vegetation fraction. During these oscillations, precipitation and vegetation adapt to each other within one decade, i.e., no time-lag is present on a decadal time-scale. The increased variability of the vegetation cover is reflected in the standard deviation, which increases from 9.2% for 9–7.5 kyr cal BP to 12.2% for 7.5–5.5 kyr cal BP. The time period separating the "green" spikes varies between 110 to 370 yr, which is comparable to the lake level fluctuations observed in high-resolution paleodata from the Western Sahara (200–500 yr, Fabre and Petit-Maire, 1988; Lézine et al., 1990). During the third phase (after 5.5 kyr cal BP), the variability decreases substantially and the system moves towards a desert state. At 1 kyr cal BP, annual precipitation is as low as 60 mm/yr and vegetation cover is only 10%.

An analysis of the monthly precipitation shows that, as expected, the difference between 9 and 0 kyr cal BP is restricted to the summer half year (Fig. 2). The early Holocene climate is particularly wetter from June to September, with a maximum in August when the 90 mm/month limit reaches up to 27°N. The maximum 9 kyr cal BP minus 0 kyr cal BP anomaly is 110 mm/month at 20°N. In this region, the overall 9–0 kyr cal BP annual precipitation reduction is more than 300 mm (Fig. 3a).

To study the nature of the instability of the AHP termination in the Western Sahara, we performed four additional sensitivity experiments of 200-yr duration (Renssen et al., 2003a). In these sensitivity experiments, we fixed in the first 100 yr the vegetation in the Sahara

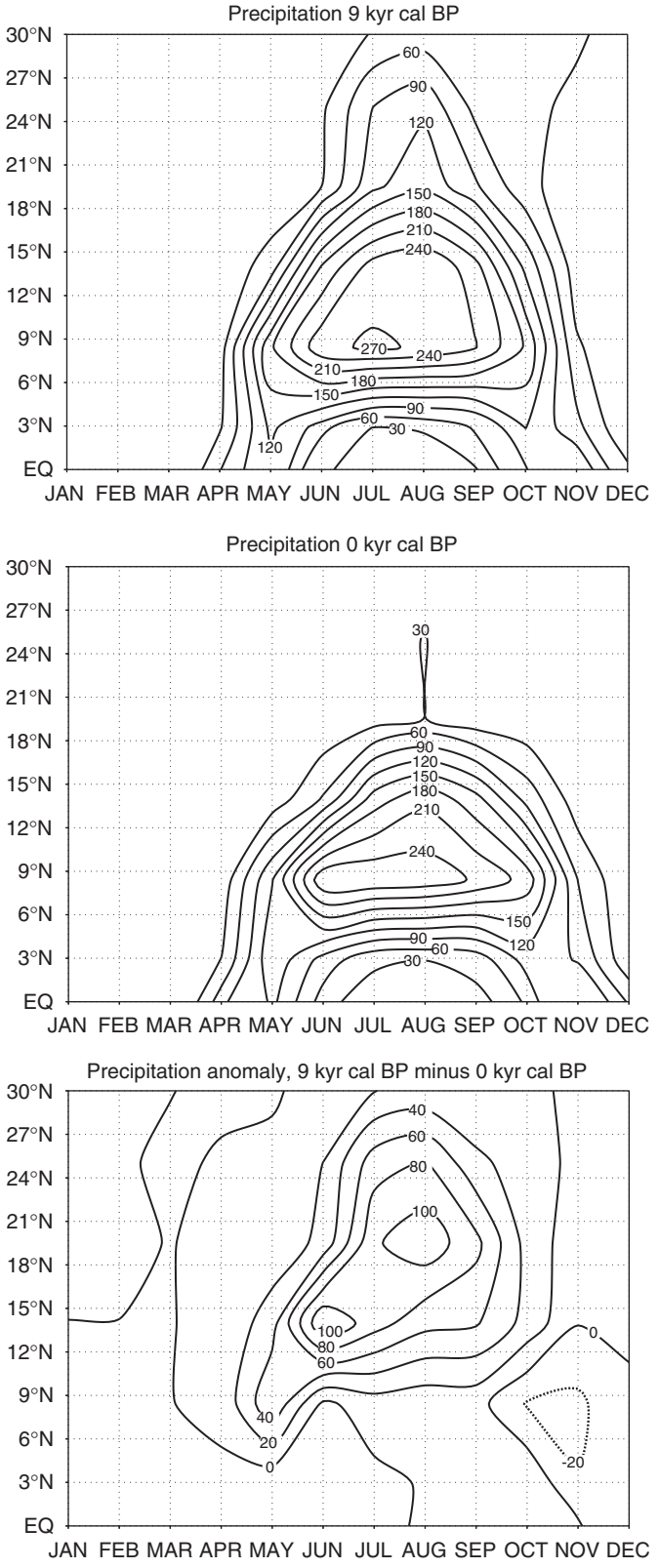

Fig. 2. (a–c) Monthly precipitation (mm/month) in the Western Sahara/Sahel plotted against latitude. Averages for the region between 10 and 0°W are also shown. (a) Top, 9 kyr cal BP, (b) middle, 0 kyr cal BP and (c) bottom, 9–0 kyr cal BP anomaly.

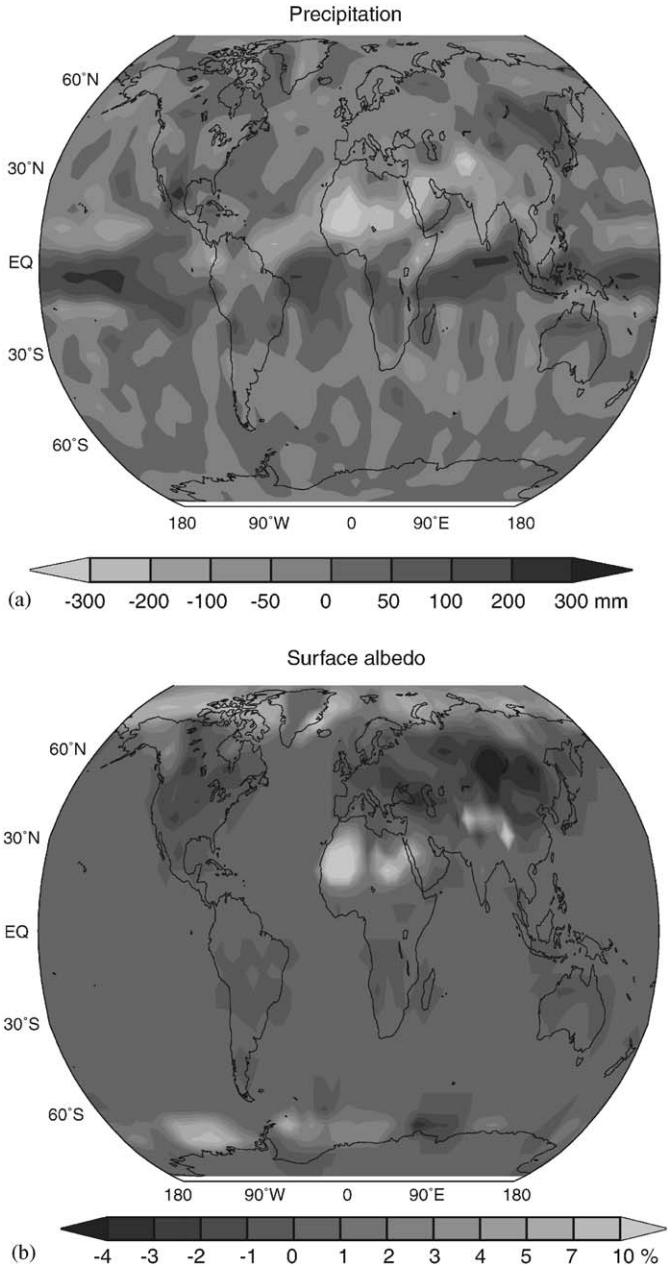

Fig. 3. (a–b) Simulated change (0 kyr cal BP minus 9 kyr cal BP) in annual precipitation (a, top, in mm/yr) and surface albedo (b, bottom, in %). The albedo anomalies over the continents are mainly related to vegetation changes, while over the oceans they mostly reflect changes in sea ice cover.

region to either 100% desert or 100% grassland, after which the vegetation model was allowed to evolve freely during the remaining 100 yr. All other forcings were kept constant at 9 kyr cal BP, 6 kyr cal BP or 0 kyr cal BP values. The four experiments can be characterized as follows: 9 kyr cal BP-desert, 6 kyr cal BP-desert, 6 kyr cal BP-green, 0 kyr cal BP-green. In the 0 kyr cal BP-green experiment, the model quickly returned to the desert state after 100 yr, showing that under present-day conditions, only the desert state is stable in our model. In the 9 kyr cal BP-desert experiment, on the other hand, the model returned to the green state, suggesting that this state is favored under 9 kyr cal BP boundary conditions. In the 6 kyr cal BP-desert and 6 kyr cal BP-green experiments, the model evolved towards an intermediate state with a vegetation cover between 45% and 60%. Thus, under 6 kyr cal BP conditions, the model has no clear preference for the green and desert states, explaining why, between 7.5 and 5.5 kyr cal BP, the stochastic variations in precipitation are able to induce transitions between the two states. These transitions are abrupt due to the effect of the biogeophysical feedback between vegetation and precipitation described by Charney (1975).

Previous climate model studies have shown that oceanic feedbacks have played a significant role in maintaining the relatively humid climate in Northern Africa in the early-to-middle Holocene (Kutzbach and Liu, 1997; Braconnot et al., 1999, 2000). Potentially, variations in surface ocean temperatures could thus have contributed to the variability in precipitation seen in our results in the Western Sahara. To study this oceanic contribution, we have conducted two additional sensitivity experiments with an identical design as 6 kyr cal BP-desert and 6 kyr cal BP-green, but without an interactive ocean (i.e., with 6 kyr cal BP sea-surface conditions prescribed to those from the CLIO model). These two experiments showed that the high-frequency variations in oceanic surface temperature are responsible for only 20% of the variability in precipitation.

According to our simulations, the succession of the discussed three phases is only characteristic for the Holocene climatic evolution in the Western Sahara. In other regions, such as the Eastern Sahara, Arabia and Western Asia, the model also simulated significant reductions in precipitation (i.e., more than 200 mm on an annual basis) and vegetation cover (as reflected by albedo changes), which are associated with the orbitally forced weakening of the summer monsoon (Fig. 3a and b). However, the changes in precipitation are not as widespread as in the Western Sahara. Moreover, simulated time-series for these regions (Fig. 4) reveal that the Western Sahara is the only area with an unstable desertification phase that is characteristic for Charney's (1975) biogeophysical feedback. Indeed, the region with the highest variability during the unstable mid-Holocene transition phase (between 7.5 and 5.5 kyr cal BP) is located in the Western Sahara (Fig. 5a–c) with the core at 20°N, 10°W (see precipitation time-series in Fig. 4). In the other regions, the precipitation reduction follows more or less linearly the trend in summer insolation (compare Fig. 1a with Fig. 4). Brovkin et al. (1998) studied the interdependence of vegetation and precipitation using a conceptual model and found that the difference in surface albedo between the desert and vegetation cover is the main factor that controls the existence of multiple states. This suggests that in regions outside the Western Sahara, no precipitation threshold is crossed in our simulation that would produce sufficiently large changes in vegetation (i.e., from grassland to desert) and surface albedo to produce a non-linear mid-Holocene transition and centennial-scale fluctuations between green and desert states.

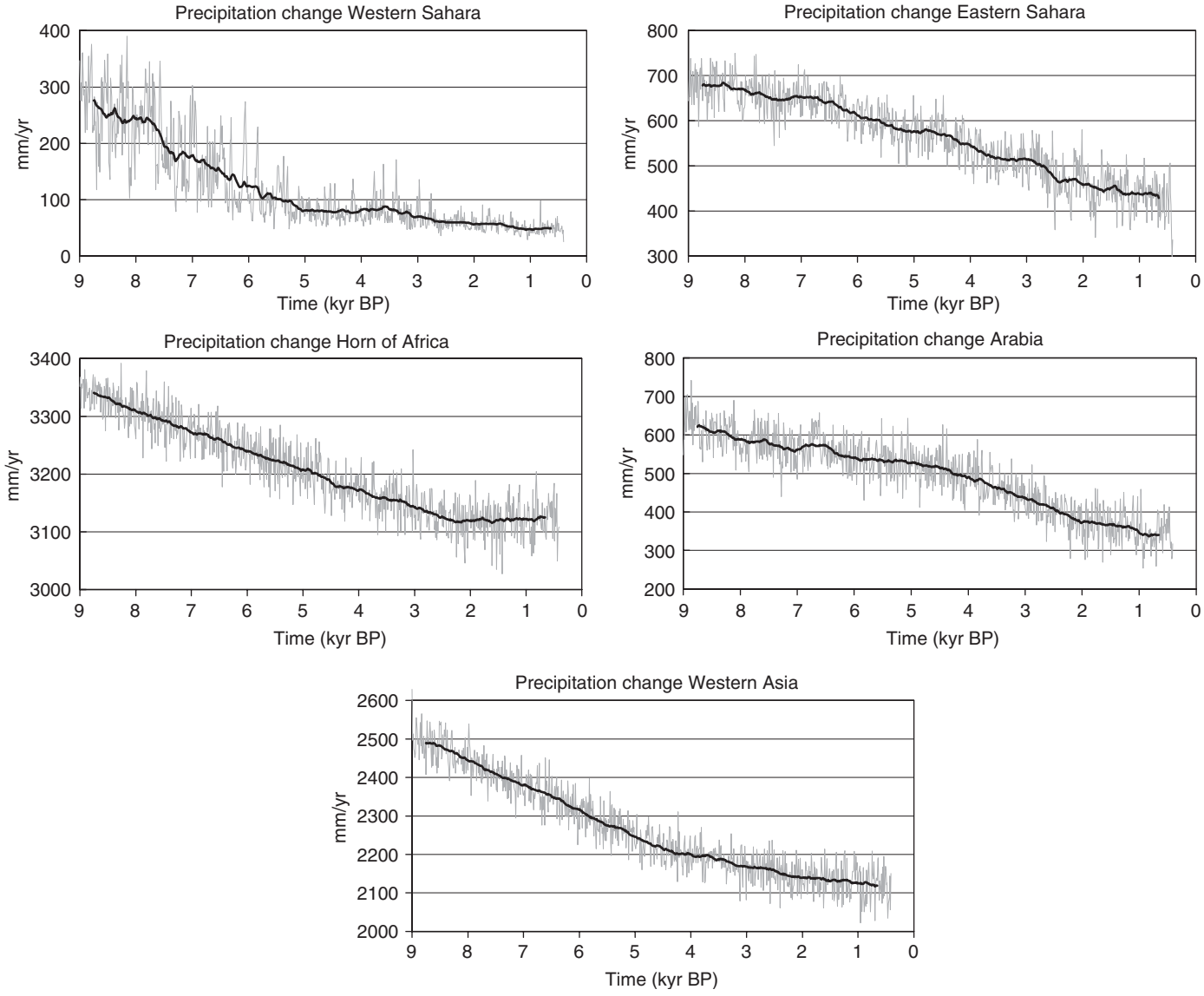

Fig. 4. Simulated precipitation changes in five different regions: Western Sahara (11°W, 19°N), Eastern Sahara (17°E, 19°N), Horn of Africa (39°E, 2°N), Arabia (39°E, 25°N) and Western Asia (73°E, 36°N). The gray curves are the decadal means, while the black thick line is the 500-point running mean.

It should be noted, however, that our model has several limitations. It has a low spatial resolution and a simplified representation of atmospheric dynamics (i.e., based on quasi-geostrophic equations) that hamper a realistic simulation of the low-latitude climate. For instance, the model has a tendency to overestimate precipitation in central North Africa, even with present-day forcings. As a consequence, the simulated 0 kyr cal BP vegetation cover at 12°E reaches 80% where desert is present in reality (Fig. 5b). In the Eastern Sahara at 25°N, on the other hand, the precipitation rates are low throughout the experiment, even at 9 kyr cal BP, so that here the 9 kyr cal BP vegetation cover is locally below 25%, while it was probably higher in the early Holocene. This implies that here the AHP termination cannot be simulated in a reliable way in our model and that the range of the simulated area with high variability (Fig. 5c) should be treated with caution. Nevertheless, in the Western Sahara, our simulation results agree with Holocene lake records (Fabre and Petit-Maire, 1988; Lézine et al., 1990) that suggest that the AHP termination was a highly unstable phase, characterized by centennial-scale fluctuations in precipitation. In the other discussed monsoonal regions, our simulation shows a less good fit with the paleoevidence. For instance, lake level records from West Asia and the Horn of Africa indicate that here the mid-Holocene wet–dry transition was possibly abrupt (e.g., Gasse and Van Campo, 1994), while our results suggest a linear Holocene evolution in line with the orbital forcing.

Another limitation of our model is that atmosphere and vegetation are only coupled via the surface albedo, thus neglecting the direct effect of changing vegetation on the evapotranspiration. A change from grassland to desert in a progressively drier climate would lead to a decrease in

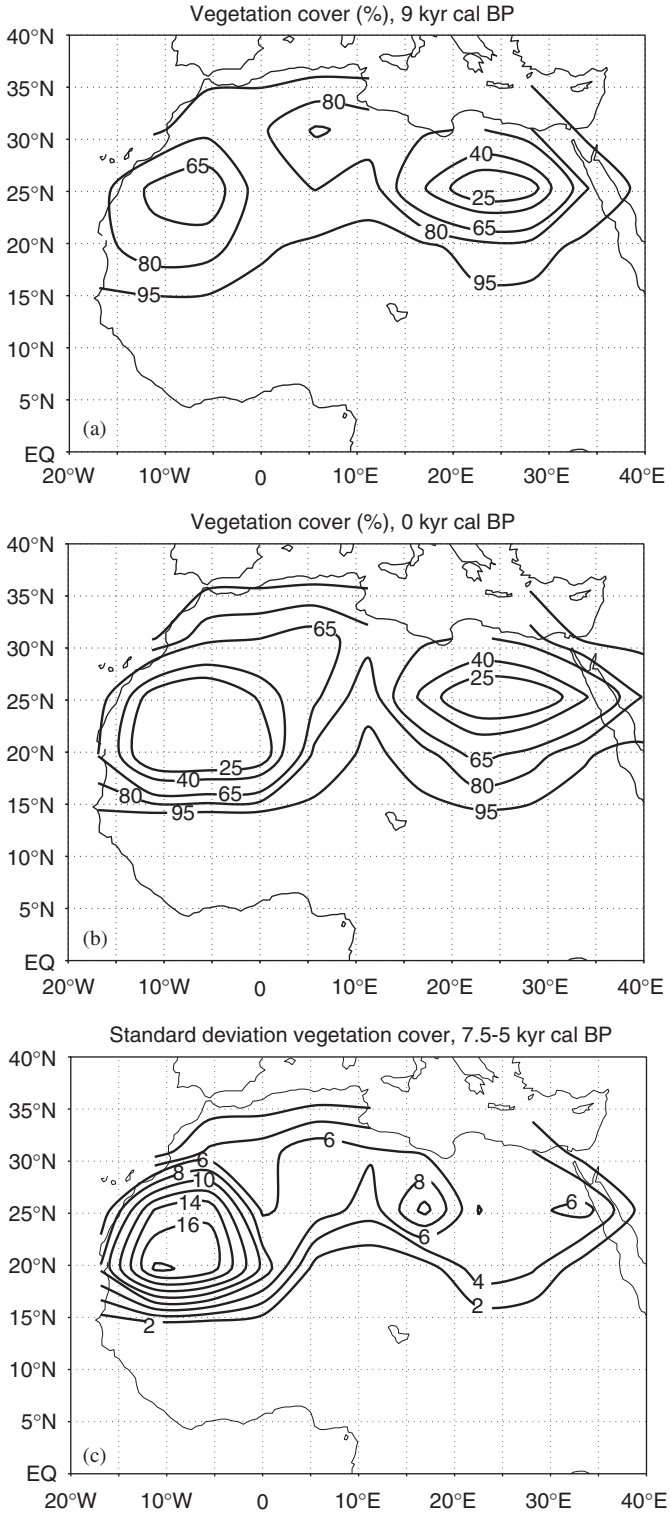

Fig. 5. (a–c) Simulated vegetation cover (%): (a) top, at 9 kyr cal BP, (b) middle, at 0 kyr cal BP and (c) bottom, standard deviation of the decadal mean during the unstable phase 7.5–5.5 kyr cal BP.

evapotranspiration, which could in turn result in lower precipitation rates (e.g., Xue and Shukla, 1993). It should be noted, however, that our model calculates part of this effect indirectly through soil moisture, as lower precipitation values lead to drier soils and hence to lower evaporation rates that feed back on local precipitation. Nevertheless, the applied simplified atmosphere–vegetation coupling could have an effect on the discussed climatic changes found in our model. Regrettably, we are not able to quantify this effect in this study.

4. Concluding remarks

Our results suggest that the Holocene evolution of the atmosphere–ocean–vegetation system in the Western Sahara may be summarized by the schematic model depicted in Fig. 6. Hypothetically, the climate–vegetation system possesses multiple steady states, desert and "green". Potential minima correspond to equilibria that are stable in the absence of perturbations. Precipitation fluctuations induced by large-scale atmospheric and oceanic variability perturb the stable state, and a positive feedback between vegetation and atmosphere amplifies external variability. Gray balls and arrows indicate the maximum range of the system variations. When the coupled atmosphere–ocean–vegetation system is forced by orbital forcing for the last 9000 yr, the following phases can be distinguished in the Western Sahara.

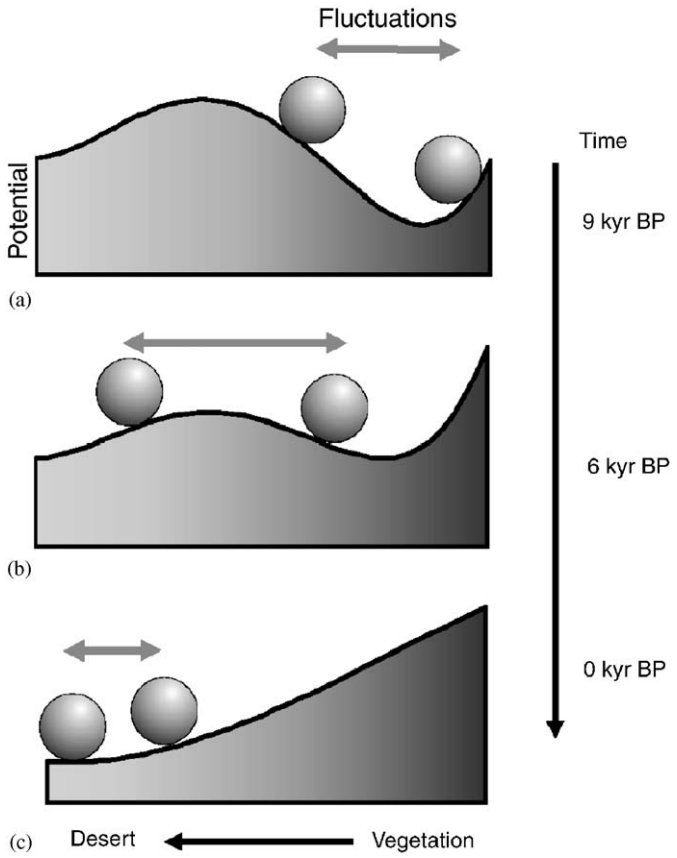

Fig. 6. Simplified cartoon of non-linear system dynamics in the Sahara/Sahel region based on experiments performed with ECBilt–CLIO–VECODE. Balls and arrows on the figure indicate maximum range of the fluctuations induced by large-scale atmospheric and oceanic variability. This is amplified by the positive feedback between atmosphere and vegetation.

(A) *9 kyr cal BP*: The dynamical system has two steady states with a preference for the green state (deeper potential minimum). The system fluctuates in vicinity of the green state.
(B) *6 kyr cal BP*: The potential became equal for both states. The system fluctuates between desert and green states with a stronger variability than at 9 kyr cal BP.
(C) *0 kyr cal BP*: After 6 kyr cal BP, the system underwent bifurcation as the green state lost stability and disappeared. Desert is now the only steady state, and the variability has decreased again. Precipitation fluctuations are reduced in comparison with the two-well system (A and B).

Similar transitions between multiple equilibria may have occurred during other orbitally forced transitions in the geological past. It should be noted that the existence of multiple stable states under particular boundary conditions is model dependent. For instance, with other models, both desert and green equilibria have been obtained for 0 kyr cal BP conditions (Brovkin et al., 1998; Claussen, 1998).

In our simulation, this sequence of events is only found in the Western Sahara region, where the conditions were ideal for the biogeophysical feedback to be effective because the precipitation rate is close to a threshold during the early Holocene. In other areas (Eastern Sahara, Western Asia, Arabia) also significant reductions in precipitation are simulated as a response to the decrease in summer insolation, but here the surface stayed covered by vegetation. Hence, in the model, the vegetation-related changes in surface albedo were insufficiently large to invoke significant variations in radiative heat loss relative to the surrounding areas and thus amplification of the reduction in precipitation. The resulting gradual reduction of precipitation in these other monsoonal regions appears in conflict with lake level data that suggest that the climate became abruptly drier in the middle Holocene (e.g., Gasse and Van Campo, 1994).

Acknowledgements

HR is supported by the Netherlands Organization for Scientific Research NWO. HG is Research Associate at the Belgian National Fund for Scientific Research. This study was carried out as a part of the Belgian Second Multi-annual Scientific Support Plan for a Sustainable Development Policy (Belgian Federal Science Policy Office, contract EV/10/9A and EV/10/7D) and the European Research Programme on Environment and Sustainable Development (European Commission, contracts EVK2-2001-00263 and EVK2-CT-2002-00153). J.M. Campin (MIT) is thanked for programming the coupling of VECODE to ECBilt and for model testing. The authors thank Ursula Werner (PIK) for technical assistance with Fig. 6.

References

Berger, A.L., 1978. Long-term variations of daily insolation and Quaternary climatic changes. Journal of the Atmospheric Sciences 35, 2363–2367.
Braconnot, P., Joussaume, S., Marti, O., de Noblet, N., 1999. Synergistic feedbacks from ocean and vegetation on the African monsoon response to mid-Holocene insolation. Geophysical Research Letters 26, 2481–2484.
Braconnot, P., Marti, O., Joussaume, S., Leclainche, Y., 2000. Ocean feedback in response to 6 kyr BP insolation. Journal of Climate 13, 1537–1553.
Brovkin, V., Claussen, M., Petoukhov, V., Ganopolski, A., 1998. On the stability of the atmosphere–vegetation system in the Sahara/Sahel region. Journal of Geophysical Research 103, 31,613–31,624.
Brovkin, V., Bendtsen, J., Claussen, M., Ganopolski, A., Kubatzki, C., Petoukhov, V., Andreev, A., 2002. Carbon cycle, vegetation and climate dynamics in the Holocene: experiments with the CLIMBER-2 Model. Global Biogeochemical Cycles 16, 1139.
Charney, J.G., 1975. Dyamics of deserts and droughts in the Sahel. Quarterly Journal of the Royal Meteorological Society 101, 193–203.
Charney, J.G., Stone, P.H., Quirk, W.J., 1975. Drought in the Sahara: a biogeophysical feedback mechanism. Science 187, 434–435.
Claussen, M., 1998. On multiple solutions of the atmosphere–vegetation system in present-day climate. Global Change Biology 4, 549–559.
Claussen, M., Kubatzki, C., Brovkin, V., Ganopolski, A., Hoelzmann, P., Pachur, H.J., 1999. Simulation of an abrupt change in Saharan vegetation in the mid-Holocene. Geophysical Research Letters 26, 2037–2040.
Damnati, B., 2000. Holocene lake records in the Northern Hemisphere of Africa. Journal of African Earth Sciences 31, 253–262.
DeMenocal, P., Ortiz, J., Guilderson, T., Adkins, J., Sarnthein, M., Baker, L., Yarusinsky, M., 2000. Abrupt onset and termination of the African humid period: rapid climate responses to gradual insolation forcing. Quaternary Science Reviews 19, 347–361.
Fabre, J., Petit-Maire, N., 1988. Holocene climatic evolution at 22–23°N from two palaeolakes in the Taoudenni area (Northern Mali). Palaeogeography, Palaeoclimatology, Palaeoecology 65, 133–148.
Gasse, F., 2000. Hydrological changes in the African tropics since the last glacial maximum. Quaternary Science Reviews 19, 189–211.
Gasse, F., Van Campo, E., 1994. Abrupt post-glacial climate events in West Asia and North Africa monsoon domains. Earth and Planetary Science Letters 126, 435–456.
Goosse, H., Fichefet, T., 1999. Importance of ice-ocean interactions for the global ocean circulation: a model study. Journal of Geophysical Research 104, 23,337–23,355.
Goosse, H., Selten, F.M., Haarsma, R.J., Opsteegh, J.D., 2001. Decadal variability in high northern latitudes as simulated by an intermediate-complexity climate model. Annals of Glaciology 33, 525–532.
Kutzbach, J.E., Liu, Z., 1997. Response of the African monsoon to orbital forcing and ocean feedbacks in the Middle Holocene. Science 278, 440–443.
Kutzbach, J.E., Street-Perrott, F.A., 1985. Milankovitch forcing of fluctuations in the level of tropical lakes from 18 to 0 kyr BP. Nature 317, 130–134.
Lézine, A.M., Casanova, J., Hillaire-Marcel, C., 1990. Across an early Holocene humid phase in Western Sahara: pollen and isotope stratigraphy. Geology 18, 264–267.
Opsteegh, J.D., Haarsma, R.J., Selten, F.M., Kattenberg, A., 1998. ECBILT: a dynamic alternative to mixed boundary conditions in ocean models. Tellus 50A, 348–367.
Prentice, I.C., Jolly, D., and BIOME 6000 participants, 2000. Mid-Holocene and glacial-maximum vegetation geography of the northern continents and Africa. Journal of Biogeography 27, 507–519.
Raynaud, D., Barnola, J.-M., Chappellaz, J., Blunier, T., Indermühle, A., Stauffer, B., 2000. The ice record of greenhouse gases: a view in the context of future changes. Quaternary Science Reviews 19, 9–17.

Renssen, H., Goosse, H., Fichefet, T., 2002. Modeling the effect of freshwater pulses on the early Holocene climate: the influence of high-frequency climate variability. Paleoceanography 17, 1020.

Renssen, H., Brovkin, V., Fichefet, T., Goosse, H., 2003a. Holocene climate instability during the termination of the African Humid Period. Geophysical Research Letters 30, 1184.

Renssen, H., Goosse, H., Fichefet, T., 2003b. On the non-linear response of the ocean thermohaline circulation to global deforestation. Geophysical Research Letters 30, 1061.

Renssen, H., Goosse, H., Fichefet, T., Brovkin, V., Driesschaert, E., Wolk, F., 2005a. Simulating the Holocene climate evolution at northern high latitudes using a coupled atmosphere–sea ice–ocean–vegetation model. Climate Dynamics 24, 23–43.

Renssen, H., Goosse, H., Fichefet, T., Masson-Delmotte, V., Koc, N., 2005b. The Holocene climate evolution in the high-latitude Southern Hemisphere simulated by a coupled atmosphere–sea ice–ocean–vegetation model. Holocene 15, 951–964.

Weber, S.L., 2001. The impact of orbital forcing on the climate of an intermediate-complexity coupled model. Global and Planetary Change 30, 7–12.

Weber, S.L., Crowley, T.J., van der Schrier, G., 2004. Solar irradiance forcing of centennial climate variability during the Holocene. Climate Dynamics 24, 539–553.

Xue, Y., Shukla, J., 1993. The influence of land surface properties on Sahel climate. Part I: Desertification. Journal of Climate 6, 2232–2245.